

Coastal Engineering Journal, Vol. 53, No. 3 (2011) 181–200
© World Scientific Publishing Company and Japan Society of Civil Engineers
DOI: 10.1142/S057856341100232X

MODELING OF SETTLING AND DEPOSITION OF SUSPENDED ORGANIC MATTER CONSIDERING BIODEGRADATION

TADASHI HIBINO* and KYUNG-HOI KIM†

*Department of Civil and Environmental Engineering, Hiroshima University,
4-1, Kagamiyama 1 chome, Higashi-Hiroshima 739-8527, Japan*

**hibinot@hiroshima-u.ac.jp*

†kobilekr@hiroshima-u.ac.jp

KENTARO NAGAO

*Institute of Environmental Informatics, IDEA Consultants, Inc.,
2-2-2 Hayabuchi Tsuzuki-ku, Yokohama 224-0025, Japan
ngo20503@ideacon.co.jp*

Received 17 November 2008

Revised 5 October 2010

To design a model for the settling of Suspended Organic Matter (SOM), the decomposition rate of organic matter, and variations in the particle size and the density of SOM were studied in the course of decomposition. The decomposition rate of SOM is estimated using the analyzed results of SOM properties (i.e. particle density, particle size, IL, and resolvability). The Multi-G Model, which formulates the decomposition of organic matter derived from phytoplankton, was chosen to calculate the decomposition rate of SOM. The parameters of each fraction in the Multi-G Model were estimated on the basis of the correlation between the deposition age and the decomposition rate of SOM. In addition, it has become possible to determine the mean decomposition rate of organic matter using the C/N ratio. Temporal variations of the particle size and the particle density of SOM during decomposition were estimated from the C/N ratio, and approximate expressions for the variations were proposed. Based on these results, it is possible to calculate the settling velocity of SOM in considering the variation of its properties due to decomposition

Keywords: Suspended organic matter (SOM); settling velocity; POC/PON (C/N ratio); decomposition.

1. Introduction

Hiroshima Bay, located in the Western Seto Inland Sea of Japan, has a low tidal exchange rate. High volumes of organic matter have been deposited as sludge due to a decrease in shoal volume and an increase in sewage inflow during Japan's rapid economic growth from 1960 to 1980. As a result, the floating mud layer has formed in extremely loose condition due to the deposition of organic matter. Furthermore, the resuspension of organic mud from the floating mud has many effects on the marine environments, such as the occurrence of eutrophication and consumption of dissolved oxygen.

The floating mud layer maintains a high water content (the maximum is over 600%), and it is verified that the resuspension of organic mud from the floating mud layer in Hiroshima Bay does not depend on the current velocity alone because the resuspension occurs even with a very slow bottom current (less than 4 cm/s) [Hibino and Matsumoto, 2006]. Consequently, it is necessary to investigate the formation of the floating mud layer (loose condition) to reveal the mechanism of resuspension of the floating mud layer.

According to Hibino and Matsumoto [2006] and Nakashita *et al.* [2007], the water content seasonally varies about several 100% in the floating mud layer due to infiltration of pore water. The ignition loss (IL) and the ratio of particulate organic carbon (POC) to particulate organic nitrogen (PON) "POC/PON ratio (C/N ratio)" also influence the water content [Kim *et al.*, 2009]. The floating mud layer consists of Suspended Organic Matter (SOM, organic matter absorbed onto fine soil particle) that reaches the sea bottom. In the course of decomposition, the organic matter changes the particle size and the density of SOM, resulting in a change in the settling velocity of SOM [Maggi *et al.*, 2007; Nishimura *et al.*, 2008]. Therefore, to clarify the condition of the floating mud layer, an analysis of the variations in SOM properties under the decomposition process is urgently required.

The purpose of this study is to propose a method for modeling the properties of SOM (derived from phytoplankton) in considering its decomposition.

2. Analysis of Settling SOM and the Sea Bottom Sediment

In order to collect the basic data related to SOM, installing sediment trap, sampling of sea bottom sediment (organic mud), and water quality observations were performed in Hiroshima Bay. SOM and sea bottom sediment were sampled at the mouth of the Ohta River (Fig. 1, St. 1 (depth: 15 m)) and Kure Bay (Fig. 1, St. 2 (depth: 20 m)). Tidal ranges in Hiroshima Bay are about 4 m and 1.5 m during the spring and neap tides, respectively.

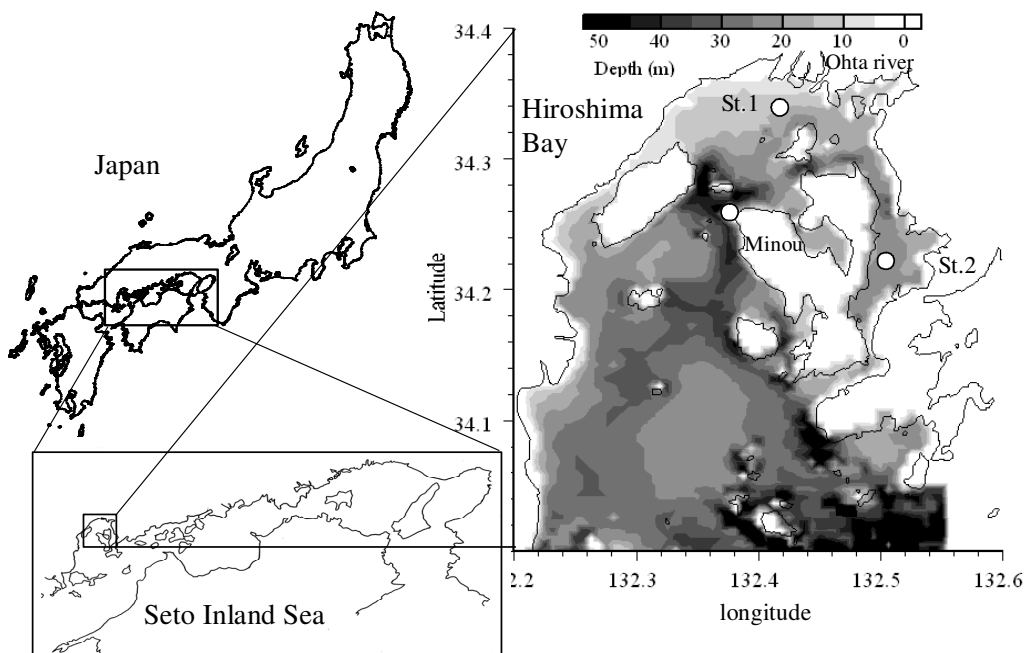


Fig. 1. Map showing the bathymetric chart and observation stations in Hiroshima Bay.

2.1. Sampling of SOM

2.1.1. Outline of the sediment trap installation

To analyze the settling and properties of SOM, sediment traps were installed at St. 1 and St. 2 (Fig. 1), from August to September in 2002, August to September 2003 (St. 2), and June to October 2005 (St. 1). Figure 2(a) shows the outline of the installation of instruments and the sediment traps in 2003 and 2004, and Fig. 2(b) shows the installation conditions in 2005. The collection and reinstallation period of the sediment trap was two weeks. Analyzed items, including the grain size distribution, SOM flux, concentrations of chlorophyll-a (Chl-a), pheophytin (Phaeo.), POC, and PON were measured and analyzed. The grain size distribution was measured using a laser diffraction particle-size distribution analyzer (Sald-2000, product of Shimadzu Corporation); and POC, PON were analyzed using “PerElmer, 2400 Series II CHNS/O System”. Chl-a + Phaeo. was analyzed using Chlorotech (AAQ1183, JEF Advantech Co. Ltd.) after diluting sediment uniformly in ultra-pure water.

2.1.2. Problems of SOM collected by the sediment trap

Generally, trapped SOM is decomposed in the sediment trap because the collection and reinstallation period is 2 weeks. It is known that decomposition of POC under aerobic is faster than under anaerobic conditions [Hibino *et al.*, 2007]. Therefore, a sediment trap was installed after deoxidizing to reduce decomposition. An anaerobic

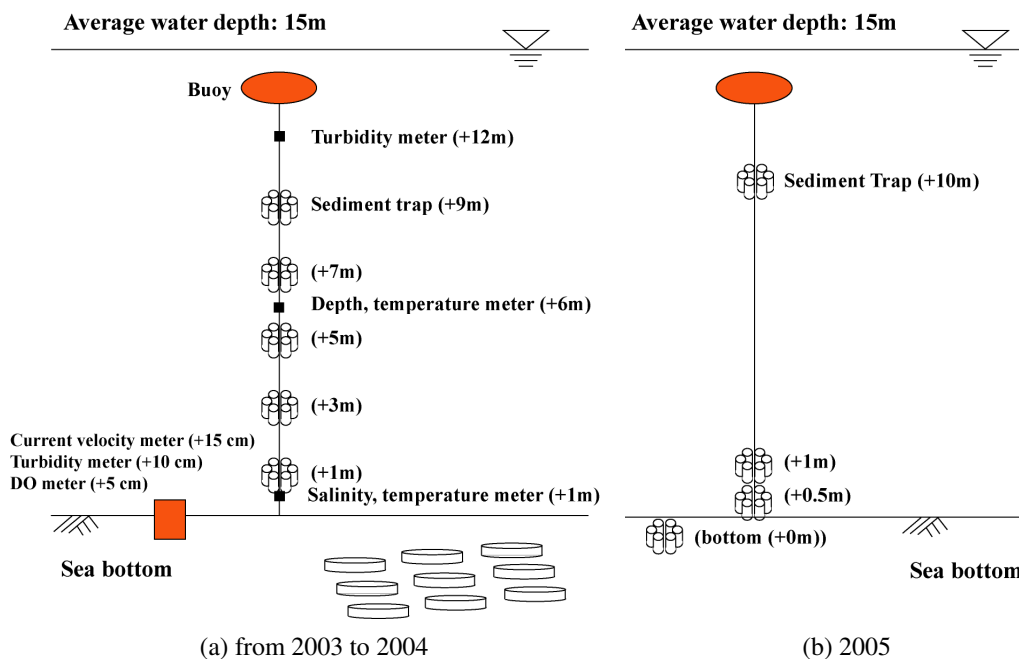


Fig. 2. Outline of sediment trap installation and water quality observations.

condition was created by bubbling N_2 gas inside a sediment trap filled with seawater before the installation. However, the decrease in amount of POC and PON cannot be ignored regardless of the experiments performed under anaerobic conditions. In this study, the subsistence (mole) ratio of C/N ratio was adopted as a result of POC and PON measurements. The C/N ratio of detritus, calculated using the equations suggested in this study (Chapter 4), increased about 0.3 (from 6.6 to 6.9) during 2 weeks under anaerobic conditions.

2.2. Sampling of the sea bottom sediment

The sea bottom sediment was sampled at St. 1 and St. 2 using a core sampler (HR TYPE CORE SAMPLER, RIGO) comprised of a cylinder, which is 110 mm in diameter and 500 mm in length. Collected samples were sliced to a thickness of 2 cm after removing overlying seawater by siphoning. Analyzed items, including the water content, wet density, IL, particle size distribution, concentrations of Chl-a, Phaeo., POC, PON, and dating were measured. The dating was carried out using the Pb_{210} method.

2.3. Water quality observation

Instruments for measuring Chl-a and turbidity (CLW meter), dissolved oxygen (DOW meter), water temperature and salinity (CT meter), and water temperature and depth (TD meter) were also installed with a sediment trap (Fig. 2(a)).

Every instrument belongs to the compact series of the ALEC Company, and the measuring time step was 10 minutes.

3. Variation of SOM Properties in the Course of Decomposition

3.1. Characteristics of flow field and water qualities

3.1.1. Hydraulic characteristics during the observation period

Figure 3 shows the time series of (a) river discharge, (b) seawater temperature, (c) salinity, (d) Chl-a, (e) turbidity and (f) current velocity at St. 1 from 6 June to 12 October 2005. Figure 4 shows the profiles of (a) the Chl-a concentration with the settling flux of Chl-a + Phaeo. and (b) the turbidity with the settling flux of SS. The numbers (e.g. [1]) in Fig. 4 indicate the installation period of the sediment trap. In this paper, the amount of Chl-a + Phaeo. is considered to be the amount of phytoplankton because the collection and reinstallation period of the sediment trap was about two weeks. Observations of the water quality and the sediment trap were stopped as a cause of a typhoon from 5 to 15 September.

Stratification formed before June and disappeared in September 2005. The seawater temperature on the sea bottom continued to increase until late September, although it stopped increasing at the surface in mid-August (Fig. 3(b)).

Salinity decreased in the flood season at Minou, which is located 10 km away from the mouth of the Ohta River. The decreasing tendency was different in July and September (Fig. 3(c)). In mid-July, low-salinity, due to the inflow of river water (the maximum river discharge is about $800 \text{ m}^3/\text{s}$), was maintained for 1 month (Fig. 3(a)). On the other hand, salinity was higher in September (the maximum river discharge is over $1000 \text{ m}^3/\text{s}$) than in July (Fig. 3(c)), whereas the maximum river discharge was relatively large in September. From these results, it appears that the current field is different in July and September, and the fresh water residence time is longer in July; the residence of low-salinity water is considered to contribute to the density stratification of seawater around St. 1 in July.

3.1.2. Temporal variation of turbidity and Chl-a on the sea bottom

The maximum turbidity on the sea bottom at St. 1 is about 20 mg/L , and the turbidity increase does not respond with increase in current velocity [Hibino and Matsumoto, 2006]. Around 10 September, when a typhoon passed, turbidity remained over 10 mg/L for 5 days, although the current velocity on the sea bottom did not increase (Figs. 3(e) and 3(f)).

The Chl-a concentration increased at St. 1 around 10 July when the river discharge was relatively large for the previous 10 days. After several days, Chl-a increased at the sea bottom (Fig. 3(d)). However, it was observed that the Chl-a increase at the sea surface did not always accompany the Chl-a increase at the sea bottom. Moreover, the SS flux was enlarged by increases in turbidity near the sea

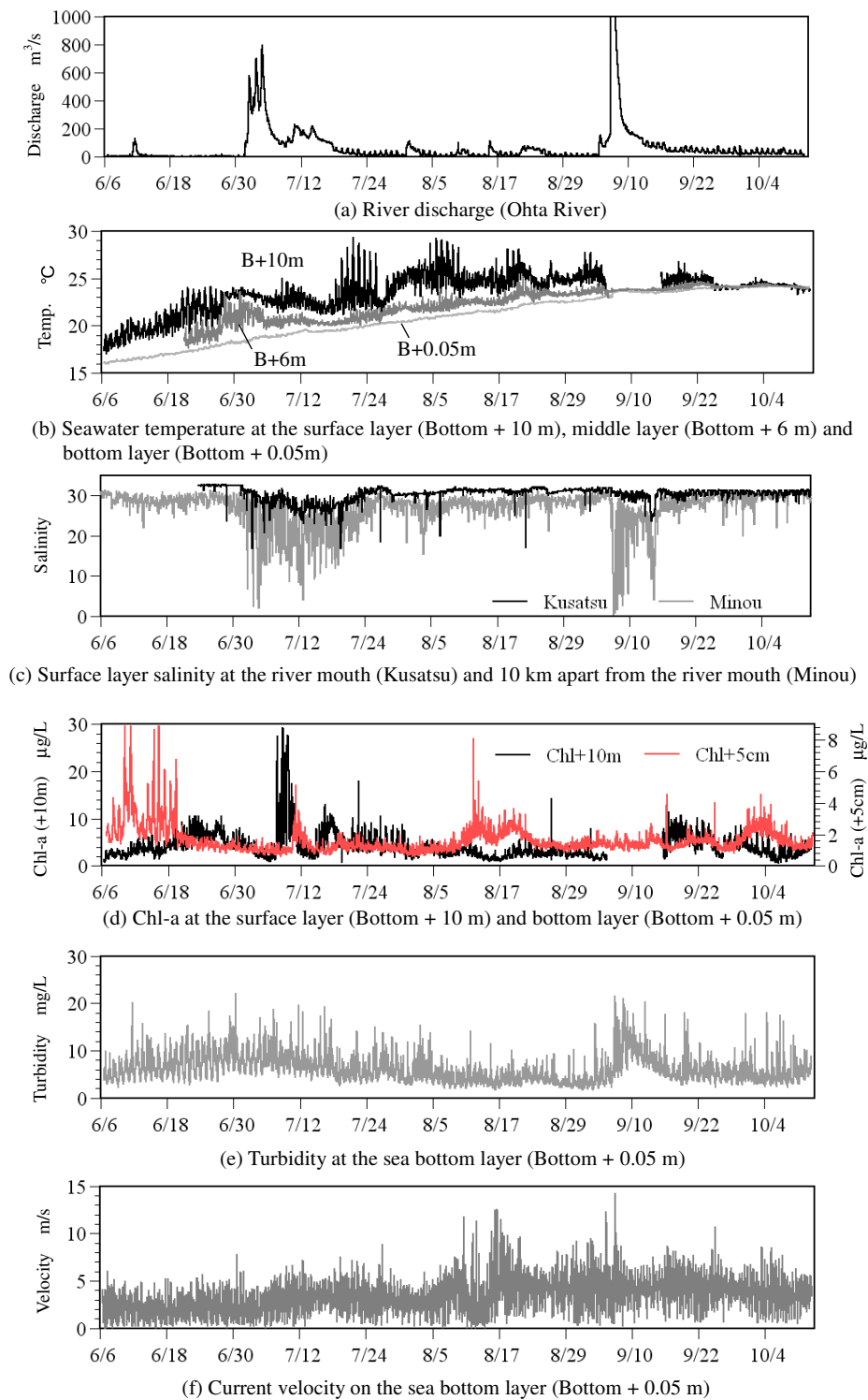


Fig. 3. Temporal variation of hydraulic characteristics at the estuary (June to October 2005).

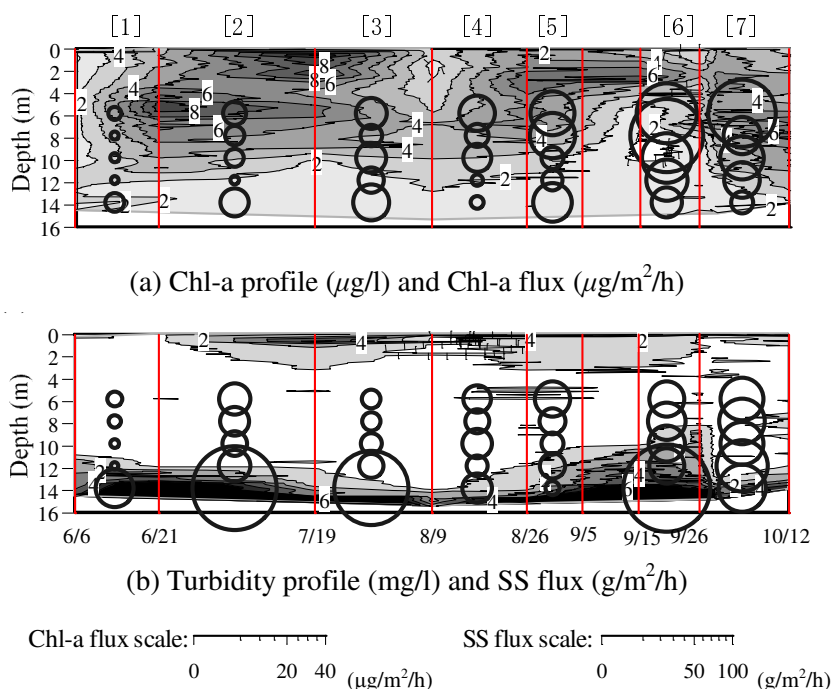


Fig. 4. Profile and flux of Chl-a and turbidity (e.g. [1]: collection period, circe: sediment traps data).

bottom (Fig. 4(b)). Thus it is considered that much of the SOM on the sea bottom is not supplied from the sea surface. Relative to this, it has been reported that 90% of SS near the sea bottom (Bottom + 1 m) is resuspended SOM from a floating mud layer in Hiroshima Bay [Sasakura *et al.*, 2005]

3.1.3. Relationship between the settling velocity and Chl-a content of SOM

The settling flux of Chl-a was small during periods [1] and [2]. It normally starts to increase in late August. Phytoplankton below a depth of 5 m is assumed to be plentiful in September and October because the Chl-a content of SOM is larger in nonstratification period ([6] and [7]) than in a stratification period. Low-salinity water accumulated near the river mouth due to the large amount of river discharge for about 15 days ([2]). The supply of nutrient salts from the Ohta River results in a high Chl-a concentration by photosynthesis in the surface sediment.

Although the Chl-a concentration was lower in periods [6] and [7] than in periods [1] and [2], SS and the Chl-a flux were relatively large during [6] and [7]. The Chl-a flux decreased with depth even though the SS flux was vertically (Bottom + 1 m–9 m) constant during [6] and [7]. These results mean that the settling velocity of SOM containing Chl-a is small during the stratification season. The adherence of Chl-a on SOM has an effect on the SOM settling velocity by variations in the particle density and the particle size.

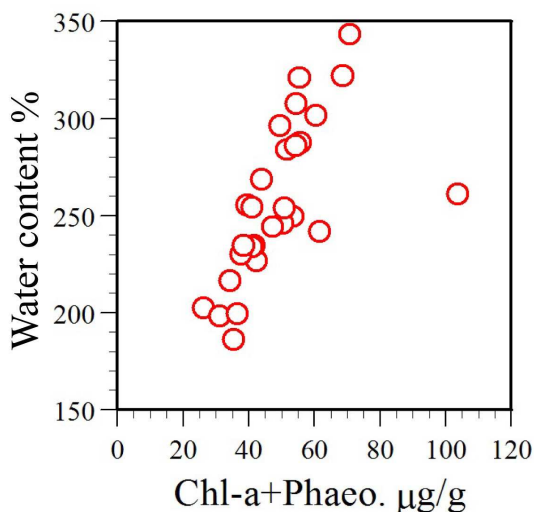


Fig. 5. Relationship between water content and Chl-a + Phaeo. of sea bottom sediment.

3.2. Characteristics of sea bottom sediment and SOM

3.2.1. Variations in the condition of the floating mud layer by settling of SOM

Figure 5 shows the relationship between the water content and Chl-a + Phaeo. content of the sea bottom sediment from 0 cm to 12 cm at St. 1. A good linear correlation was observed in the data with one exception. Generally, Chl-a and Phaeo. are derived from the sea surface. The C/N ratio of the sea bottom sediment was reduced by the deposition of fresh SOM (Chl-a), which resulted in the decrease in the water holding capacity of SOM. Thus, it is thought that the transportation of Chl-a into the sea bottom sediment by pore water flow plays a role to make high water content of sea bottom sediment (especially floating mud layer).

3.2.2. Properties of SOM derived from primary production

The IL and C/N ratio affect the particle size and the particle density of SOM [Nakashita *et al.*, 2007]. In this section, in order to understand the variations in the particle size and the particle density of SOM, variations in the SOM properties were analyzed.

(1) Seasonal variation of SOM properties

Figure 6 shows the temporal variations in (a) (Chl-a + Phaeo.)/SS, (b) the C/N ratio, (c) IL, and (d) POC/(Chl-a + Phaeo.) of SOM at 5 depths shown in Fig. 2(a).

The C/N ratio and POC/(Chl-a + Phaeo.) tend to decrease with an increase in Chl-a + Phaeo./SS, whereas (Chl-a + Phaeo.)/SS tend to decrease with depth in this period.

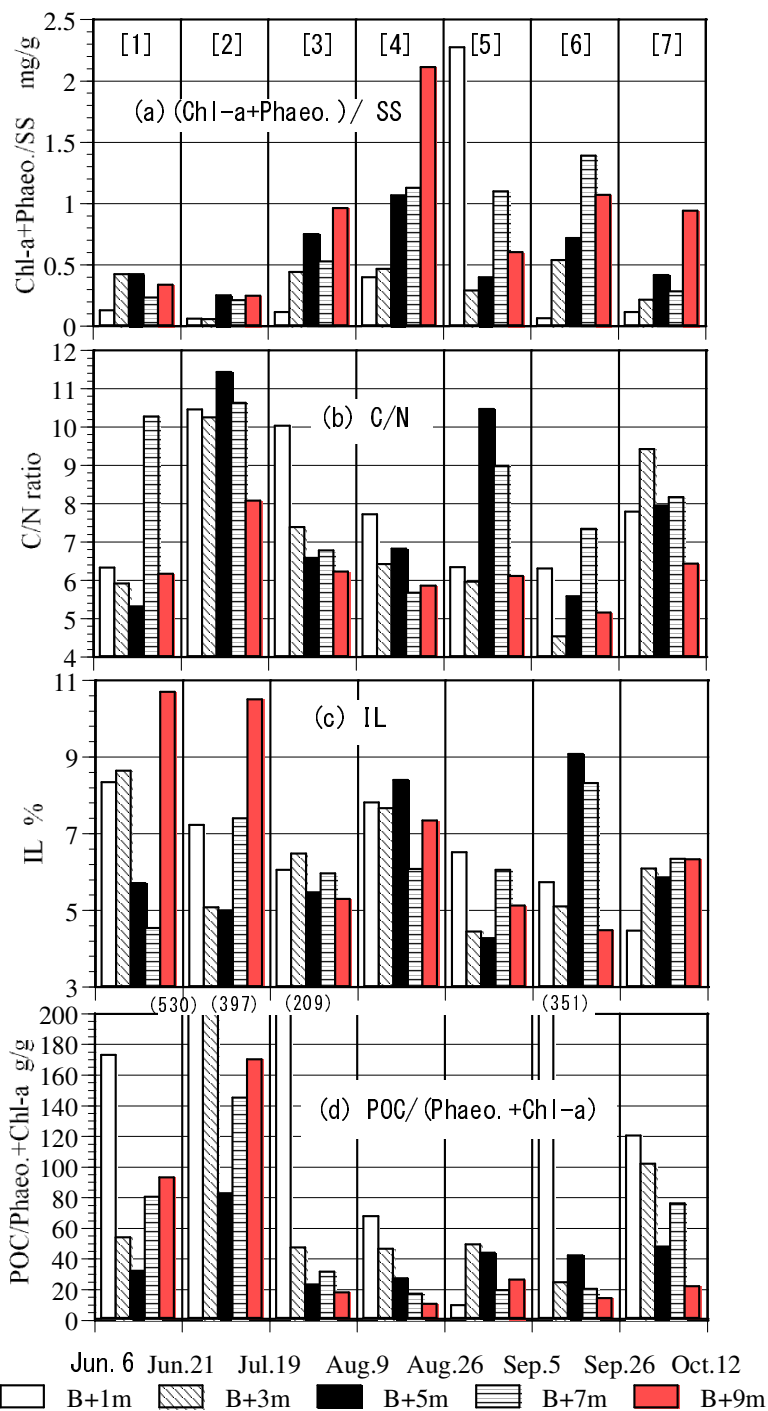


Fig. 6. (a) Content of Chl-a, Phaeo., (b) C/N ratio, (c) Ignition Loss, and (d) POC/(Chl-a + Phaeo.) ratio of the settling matter in the sediment trap. Dates indicate installation and recovery. Numbers in the legend are installation height from the sea bottom; numbers in parentheses are values that exceed the axis; and the B + number is the distance (number) from the sea bottom.

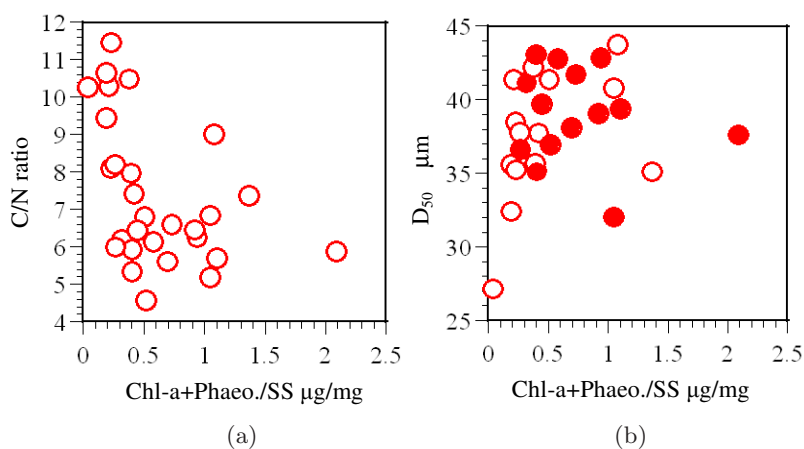


Fig. 7. Relationship between (a) the amount of Chl-a and C/N ratio and (b) the amount of Chl-a and particle size (●: mean C/N is less than 7).

IL ranged from 4% to 11%, and the IL variation depended on the amount of Chl-a after mid-July. This result shows that SOM contains more of organic matter than Chl-a before mid-July. POC/(Chl-a + Phaeo.) ranged from 10 mg/g to 20 mg/g at the surface layer, and from 20 mg/g to 40 mg/g in a layer below the surface when the primary production is active.

(2) Relationship among SOM properties

Figure 7 shows the relationship between (a) (Chl-a + Phaeo.)/SS and the C/N ratio of SOM and (b) (Chl-a + Phaeo.)/SS and D_{50} of SOM at all layers where the sediment trap was installed. The solid circles in Fig. 7 indicate the data whose C/N ratio is below 7.

The increase of (Chl-a + Phaeo.)/SS accompanies the decrease in the C/N ratio and increase in D_{50} . The high Chl-a content and the large particle size are assumed to be characteristics of SOM trapped near the sea surface because SOM forms by adherence of phytoplankton detritus onto fine soil particles [Nishimura *et al.*, 2008].

The C/N ratio of phytoplankton is about 6.6 and SOM, which has a C/N ratio below 6.6, is considered to be formed by adherence of other kinds of organic matter besides Chl-a. The analysis of this organic matter remains an intense topic of study. In this paper, it is assumed that organic matter has the same decomposition process.

3.3. Understanding the SOM settling process

The settling velocity of SOM is dependent on the particle density and size. However, they are varied by the decomposition of organic matter during settling. In this section, variations in the particle density and size of SOM relating to the decomposition in the course of settling are discussed.

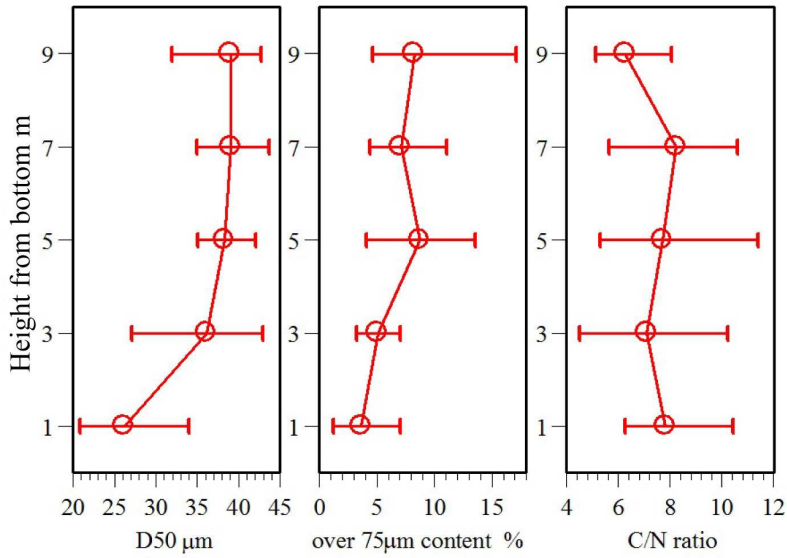


Fig. 8. Vertical distribution of D_{50} , contents of over 75 μm particle and C/N ratio (\circ : average of 7 observations).

3.3.1. Variations in the SOM properties by the decomposition in the course of settling

Figure 8 shows the vertical distributions of D_{50} , coarse particle content (over 75 μm), and C/N ratio, which were analyzed using the sample collected by sediment traps. D_{50} and the coarse particle content were relatively large in the upper layers and decreased with depth. On the contrary, the C/N ratio was at its minimum on the surface layer and increased with depth. The C/N ratio at the surface layer ranged from 4 to 8, and its average was close to the Redfield ratio. On the other hand, the C/N ratio increased to 6–11 below the surface; that is to say, the organic matter decomposes during settling.

3.3.2. Variations in the particle density and particle size of SOM and its effect on the settling velocity

(1) Apparent settling velocity of SOM

The settling velocity w' , which is affected by the vertical current velocity and settling velocity, was measured by the SOM concentration (C_0) around the sediment trap and the settling flux (F), as expressed in Eq. (1). Here C_0 is the turbidity observed when the sediment trap was installed:

$$w' = \frac{F}{C_0} = \frac{R - C_0 V}{AT} \frac{1}{C_0}, \quad (1)$$

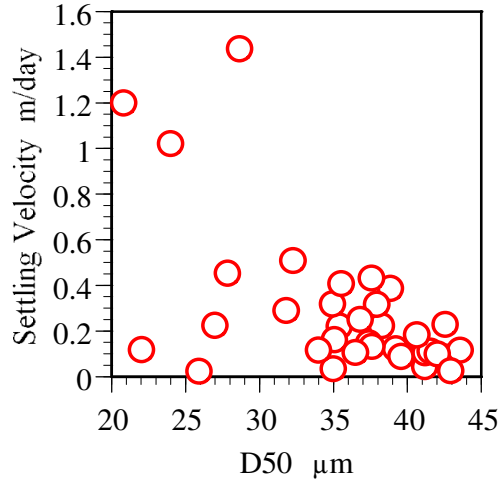


Fig. 9. Relationship between D_{50} and settling velocity of SOM.

where R is the amount of trapped SOM (g), V is the volume of the sediment trap (cm^3), A is the area of the sediment trap opening (cm^2), and T is the experimental period (day).

(2) *Estimation of the particle density of SOM*

Variations in the particle density and size by the adherence and decomposition in SOM are considered to influence the settling velocity.

The relationship between the apparent settling velocity w' calculated using Eq. (1) and D_{50} is shown in Fig. 9. Usually, the settling velocity is proportional to the particle size. However, the settling velocities of SOM, especially, the large D_{50} were in inverse proportion to the particle size as shown in Fig. 9. From this result, it is thought that the particle density plays an important role in estimating the settling velocity of SOM.

It is difficult to measure the particle density of SOM directly. Therefore, the particle density was calculated using the following method. First, the settling velocity w is derived from Stokes Law, as shown in Eq. (2a):

$$w = \frac{4g}{135} \frac{(\rho_s - \rho)}{\mu} d^2, \quad (2a)$$

where ρ_s is the SOM density (g/cm^3), ρ is the seawater density (g/cm^3), d is the particle size of SOM (mm), and μ is the viscosity coefficient ($\text{kg}/\text{s}/\text{m}^2$).

Equation (2a) could be transformed into Eq. (2b) by substitution of the measured w' and D_{50} into w and d , respectively. The density difference ρ_e between SOM and seawater was calculated using Eq. (2b):

$$\rho_e = \rho_s - \rho = \frac{135\mu \cdot w'}{4gD_{50}^2}. \quad (2b)$$

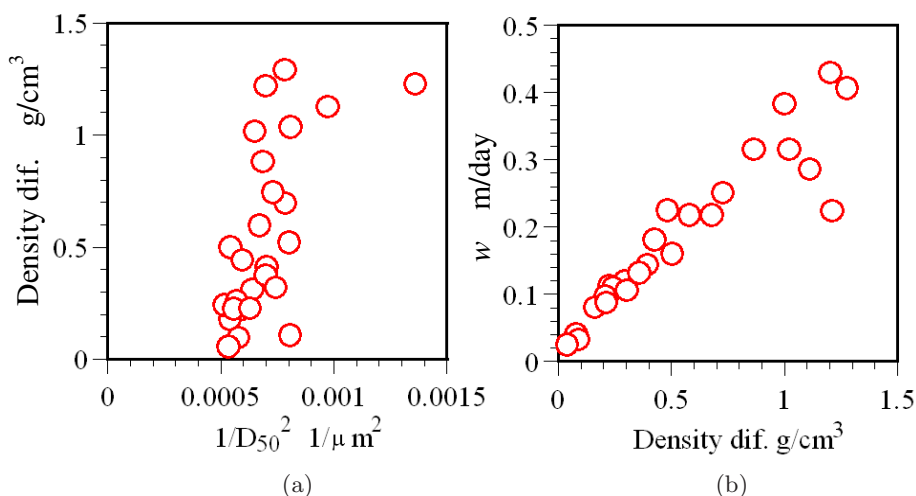


Fig. 10. Relationship between (a) density difference (seawater and SOM) and D_{50} and (b) density difference (seawater and SOM) and settling velocity.

Figure 10(a) shows the relationship between the density difference (ρ_e) and $1/D_{50}^2$. It is possible to make a proportional relationship between the density difference and the settling velocity because the observed results of $1/D_{50}^2$ have a relatively small variation range that is unrelated to ρ_e . As a result, it is possible to calculate the settling velocity of SOM from the density difference using the relation in Fig. 10(b), if the density difference (effective density) (ρ_e) is known.

4. Modeling of the SOM Settling Process

4.1. *Decomposition model of organic matter in SOM derived from primary production*

Phytoplankton detritus, adhering to fine soil particles in the sea surface layer, settle at the sea bottom. At the same time, the properties of SOM are affected by organic matter decomposition. In general ecological modeling, the decomposition of organic matter is expressed by the Simple-rate Model (Eq. (3)):

$$O_T(t) = O_0 \cdot [\exp(-kt)], \quad (3)$$

where t is the elapsed time, $O_T(t)$ is the concentration of organic matter after t , O_0 is the initial concentration of organic matter, and k is the coefficient of decomposition rate.

However, it is difficult to estimate the decrease in organic matter (e.g. POC or PON) by decomposition using the Simple-rate Model because organic matter derived from primary production consists of several kinds of fractions, which have different decomposition rates.

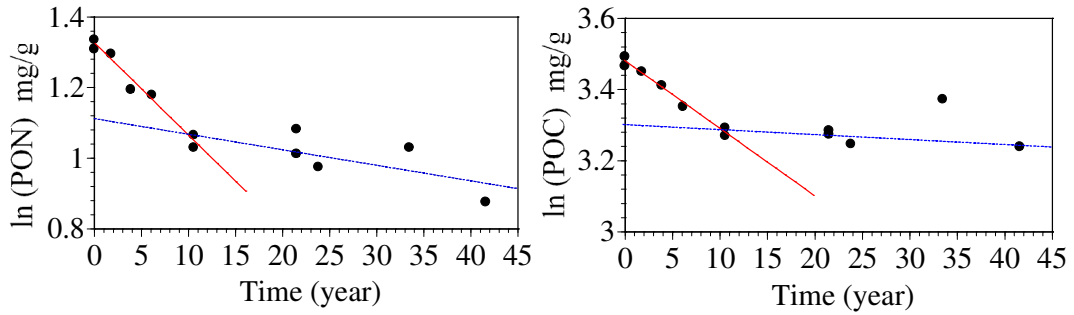


Fig. 11. Concentrations of PON and POC in anoxic sediment plotted against time. The solid line indicates the decomposition rate of the slow-labile fraction and the refractory fraction, and the dotted line indicates the decomposition rate of the refractory fraction.

4.1.1. Formulation of decomposition process of organic matter

There is a negative correlation between age and the decomposition rate of organic matter in SOM derived from primary production. Westrich and Berner [1984] have proposed Eq. (4), which is called the Multi-G Model. This equation calculates the decomposition amount of organic matter by dividing organic matter into a fast-labile fraction, a slow-labile fraction, and a refractory fraction based on different decomposition rates:

$$O_T(t) = O_{01}[\exp(-k_1t)] + O_{02}[\exp(-k_2t)] + O_{NR}, \quad (4)$$

where O_{01} , O_{02} , and O_{NR} stand for the fast-labile, the slow-labile, and the refractory fraction, and k_1 and k_2 are the decomposition parameters of the fast-labile fraction and the slow-labile fraction, respectively.

Each fraction in organic matter influences the process of the dissolution of nutrient salts from the sea bottom sediment. Thus, it is necessary to clarify the composition ratio of each fraction (O_{01} , O_{02} , O_{NR}) in organic matter.

4.1.2. Estimation of model parameters associated with the decomposition of organic matter

To estimate the parameters of the decomposition rate of organic matter, analyses of the vertical distribution of POC, PON concentrations and dating of the sea bottom sediment were carried out. The deposited period (dating) was estimated using the Pb_{210} method. Figure 11 shows temporal variations of the PON and POC concentrations in the sea bottom sediment sampled at St. 2. Figure 12 shows the relationship between the PON concentration and the C/N ratio of SOM.

The C/N ratio of the sea bottom sediment exceeded 10 because the fast-labile fraction, which has high resolvability, is exhausted during settling or before accumulating on the surface of the sea bottom (Fig. 12). As a result, the decomposition process of organic matter in the sea bottom sediment can be controlled by only two

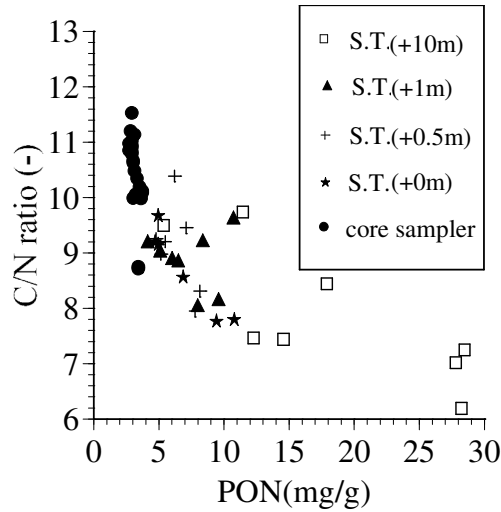


Fig. 12. Relationship between the C/N ratio and PON of SOM.

fractions. Using Eq. (4), the decomposition process of PON and POC in the sea bottom sediment is expressed by Eqs. (5a) and (5b), respectively:

$$N_T(t) = N_{02}[\exp(-k_{02}t)] + N_{NR}[\exp(-k_{NR}t)], \quad (5a)$$

$$C_T(t) = C_{02}[\exp(-k_{02}t)] + C_{NR}[\exp(-k_{NR}t)], \quad (5b)$$

where N_{02} , and N_{NR} stand for the slow-labile, and the refractory fraction of Nitrogen, C_{02} and C_{NR} stand for the slow-labile, and the refractory fraction of Carbon, and k_{02} and k_{NR} are the decomposition parameters of the slow-labile fraction and the refractory fraction, respectively.

From the gradient of lines in Fig. 11 the k_{02} of PON and POC is estimated to be 0.18 day^{-1} and 0.17 day^{-1} , and the k_{NR} of PON and POC is estimated to be 0.0025 day^{-1} and 0.0007 day^{-1} , respectively. According to Nakamura *et al.* [1996], the sea bottom sediment is under an anaerobic condition except for the 2 mm of surface layer. Thus, these parameters are valid under the anaerobic condition.

4.1.3. Compartmentalizing of each fraction in organic matter

In Fig. 12, the PON concentration tends to decrease with depth, whereas the C/N ratio increases because the decomposition rate of low C/N organic matter is higher. Thus, the composition ratio of each fraction could be calculated from the C/N ratio using Eqs. (6) to (9) as follows.

Equation (6) indicates the Redfield ratio:

$$\frac{C_T(0)}{N_T(0)} = \frac{C_{01} + C_{02} + C_{NR}}{N_{01} + N_{02} + N_{NR}} = 6.625. \quad (6)$$

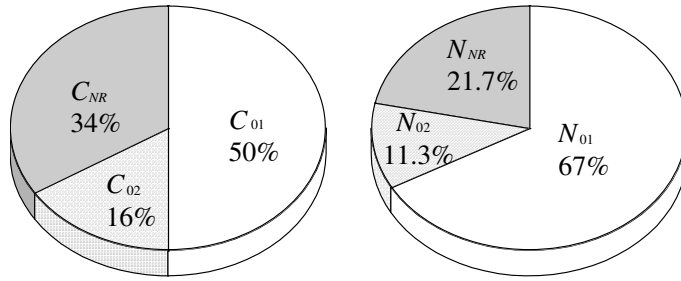


Fig. 13. Composition ratio of each fraction in SOM from primary production (Composition ratio of POC is calculated by the equations proposed by Westrich and Berner [1984]).

Most of the refractory fraction is decomposed in the sea bottom sediment because of the low decomposition ratio. Equation (6) (the C/N ratio of refractory fraction) is calculated from the intercepts of the broken line after converting the weight ratio into a mole ratio, shown in Fig. 11:

$$\frac{C_{NR}}{N_{NR}} = 10.4. \quad (7)$$

The C/N ratio of organic matter tends to increase with depth by the decomposition of the fast-labile fraction, and the maximum C/N ratio is about 10 (Fig. 12). On the other hand, the C/N ratio of the sea bottom sediment exceeded 10. As a result, a C/N ratio of 10 is assumed to be the reference point marking the existence of the fast-labile fraction. On the assumption that only the fast-labile fraction decomposes during settling, the C/N ratio of the slow-labile fraction (O_{O2}) and the refractory fraction (O_{NR}) without decomposition is about 10.1. From these results, it is possible to estimate the C/N ratio of organic matter except for the fast-labile fraction (Eq. (8)):

$$\frac{C_{O2} + C_{NR}}{N_{O2} + N_{NR}} = 10.1. \quad (8)$$

The composition ratio of each fraction in POC of phytoplankton was estimated by Westrich and Berner [1984] (Eq. (9)):

$$C_{O1} = 0.50 \cdot C_T(0), \quad (9a)$$

$$C_{O2} = 0.16 \cdot C_T(0), \quad (9b)$$

$$C_{NR} = 0.34 \cdot C_T(0). \quad (9c)$$

The composition ratio of each fraction in organic matter derived from primary production was calculated using Eqs. (6)–(9), and shown in Fig. 13. The coefficient of the decomposition rate from culture tests in aerobic conditions, examined by Aizaki and Takamura [1991], is adopted for parameters concerning the decomposition rate of the fast-labile fraction. The parameters of the decomposition rate of PON and

Table 1. Parameters of decomposition rate of PON and POC.

1/year (0°C)	Nitrogen			Carbon		
	$K_{N,01}$	$K_{N,02}$	$K_{N,03}$	$K_{C,01}$	$K_{C,02}$	$K_{C,03}$
Oxic	19.0	—	—	23.0	—	—
Anoxic	—	0.053	0.00074	—	0.050	0.00021

POC are shown in Table 1. The decomposition rate is expressed as a function of the temperature (Eq. (10)):

$$k^{0^\circ\text{C}} = \frac{k^{\text{Temp}}}{\alpha}, \quad \alpha = \exp(0.0697 \cdot \text{Temp}), \quad (10)$$

where subscript Temp is the temperature of seawater or the sea bottom sediment. It is assumed that the decomposition of the sea bottom sediment (Fig. 11) corresponds to the mean seawater temperature at the observation station during 20 years.

From these results, it is possible to quantify the mean decomposition rate using the C/N ratio and the composition rate of each fraction.

4.2. Modeling of the SOM settling process considering decomposition

4.2.1. Model concepts

The settling process of SOM is modeled on the basis of the following concepts:

- (1) The properties of organic matter in SOM vary by decomposition.
- (2) Variations in the particle density and size represent variation in the SOM properties.
- (3) The decomposition of SOM starts after the formation of SOM and could be calculated by the Multi-G Model.
- (4) The settling velocity of SOM is determined as a function of the particle size, the density of SOM, and the seawater density (the governing equation is Stokes Law).

4.2.2. Proposal a method for modeling the decomposition process of SOM

Temporal variations in the amount of organic matter and the C/N ratio of SOM by decomposition are calculated using the Multi-G Model (as shown in Eq. (11)):

$$C_T(t) = C_1[\exp(-k_{C,1}t)] + C_2[\exp(-k_{C,2}t)] + C_3[\exp(-k_{C,3}t)], \quad (11a)$$

$$N_T(t) = N_1[\exp(-k_{N,1}t)] + N_2[\exp(-k_{N,2}t)] + N_3[\exp(-k_{N,3}t)], \quad (11b)$$

where C_T is the total POC and N_T is the total PON in phytoplankton, k_i is the parameter of the decomposition rate, C_i is POC, N_i is PON, and i ($= 1, 2, 3$) denotes the fast-labile fraction, the slow-labile fraction, the refractory fraction, respectively.

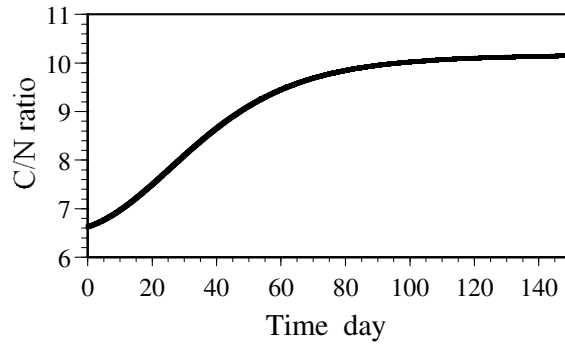
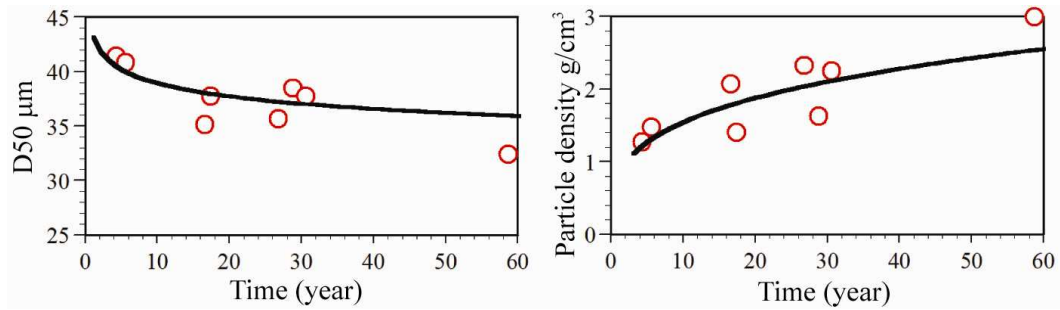


Fig. 14. Temporal variation in the C/N ratio by decomposition.

Fig. 15. Temporal variations of particle size (D_{50}) and density of SOM by decomposition (o: observed data, solid line: an approximate curve).

The Redfield ratio (6.625) is adopted as the initial C/N ratio of SOM. The composition ratio of each fraction in SOM is shown in Fig. 13. Generally, the deposition of organic matter during settling occurs under aerobic conditions. Pereira *et al.* [1994] insists that the decomposition rate under aerobic conditions is three times faster than that under anaerobic conditions. Thus, the parameters for aerobic conditions were set by three times the parameters for anaerobic conditions (Table 1).

Figure 14 shows temporal variations of the predicted C/N ratio of SOM using Fig. 13 and Eq. (11). The age of SOM sampled by sediment traps was estimated from their C/N ratio based on the relation shown in Fig. 14. The relationship of the estimated age with the particle size (D_{50}) and density (ρ_s) is shown in Fig. 15. Decomposition of organic matter accompanies the decrease in the particle size and increase in the particle density of SOM. From these results, the temporal variations of the particle size and density of SOM were formularized in Eqs. (12a) and (12b). It is possible to calculate the settling velocity of SOM by substituting Eqs. (12a) and (12b) into Eq. (10):

$$D_{50} = D_{50b} \cdot t^{-0.045}, \quad (12a)$$

$$\rho_s = \rho_{sb} \cdot t^{0.28}, \quad (12b)$$

where D_{50b} is the initial median diameter of particle, ρ_{sb} is the initial particle density, and t is the elapsed time after formation (day). $D_{50b}(43 \mu\text{m})$ and $\rho_{sb}(0.8 \text{ g/cm}^3)$ are adopted from Fig. 15.

5. Conclusions

To propose a method for modeling the SOM settling process, modeling of the organic matter decomposition and variations in the particle size and density of SOM related to the decomposition were analyzed. From this study, the following conclusions could be made:

- (1) It was suggested that the particle density of SOM could be estimated by Stokes Law. An increase of the Chl-a content in SOM decreased the particle density and enlarged the particle size.
- (2) Determination of the parameters in the Multi-G Model, which formulates the decomposition process of organic matter derived from phytoplankton, was performed. The parameters of each fraction were estimated on the basis of the correlation between the deposition age and the decomposition rate. From these results, it is possible to estimate the mean decomposition rate of organic matter using the C/N ratio.
- (3) The age of SOM collected by the sediment trap was predicted from the C/N ratio using the Multi-G Model. The temporal variations of D_{50} and density of SOM during settling were estimated and an approximate expression for the variations was proposed. Based on these results, it is possible to calculate the settling velocity of SOM in considering its property variation due to decomposition.

References

- Aizaki, M. & Takamura, N. [1991] "Regeneration of nutrient and detritus formation from aerobic decomposition of natural phytoplankton," *Jpn. J. Limnol.* **52**, 83–94.
- Hibino, T. & Matsumoto, H. [2006] "Distribution of the fluid mud layer in Hiroshima Bay and its seasonal variation," *Coast. Environ. Eng.* **63**, 348–359 (in Japanese).
- Hibino, T., Nishimura, H., Komai, K. & Matsunaga, Y. [2007] "Study on settling model of suspended organic matter in coastal region," *Coast. Environ. Eng.* **54**, 1181–1185 (in Japanese).
- Kim, K. H., Abe, M., Komai, K. & Hibino, T. [2009] "The effect of pore water infiltration on the resuspension of sea bottom sediment," *Annu. J. Coast. Eng.* **56**, 917–975 (in Japanese).
- Maggi, F., Mietta, F. & Winterwerp, J. C. [2007] "Effect of variable fractal dimension on the floc size distribution of suspended cohesive sediment," *J. Hydrol.* **343**, 43–55.
- Nakamura, Y., Inoue, T., Fatos, K. & Sayama, M. [1996] "Bisyosansodenkyokuo Motiita Nodokyokaisono Bisaikouzono Haaku," *Annu. J. Coast. Eng.* **43**, 1081–1085 (in Japanese).
- Nakashita, S., Kim, K. H., Hibino, T. & Matsunaga, Y. [2007] "The characteristics of organic matters circulation in Hiroshima Bay," *Proc. Asian and Pacific Coasts*, pp. 2051–2062.
- Nishimura, H., Komai, K., Imagawa, M. & Hibino, T. [2008] "Studies on formation of suspended organic matter — Adsorption characteristics of organic matter," *Annu. J. Coast. Eng.* **55**, 1056–1060 (in Japanese).

- Pereira, A., Tassin, B. & Jørgensen, S. E. [1994] "A model for decomposition of the drown vegetation in an Amazonian reservoir," *Ecol. Model.* **75/76**, 447–458.
- Sasakura, S., Hibino, T., Takamido, R., Murakami, K. & Matsumoto, H. [2005] "Setting process of suspended particulate matter in Hiroshima Bay," *Annu. J. Coast. Eng.* **52**, 911–915 (in Japanese).
- Westrich, J. T. & Berner, R. A. [1984] "The role of sedimentary organic matter in bacterial sulfate reduction: The G model tested," *Limnol. Oceanogr.* **29**(2), 236–249.